

## Stacking Variants and Superconductivity in the Bi–O–S System

W. Adam Phelan,<sup>†,||</sup> David C. Wallace,<sup>†,||</sup> Kathryn E. Arpino,<sup>†,||</sup> James R. Neilson,<sup>†,||</sup> Kenneth J. Livi,<sup>§</sup> Che R. Seabourne,<sup>‡</sup> Andrew J. Scott,<sup>‡</sup> and Tyrel M. McQueen<sup>\*,†,||</sup>

<sup>†</sup>Department of Chemistry, <sup>||</sup>Department of Physics and Astronomy, Institute for Quantum Matter, and <sup>§</sup>Department of Earth and Planetary Sciences, Johns Hopkins University, Baltimore, Maryland 21218, United States

<sup>‡</sup>Institute for Materials Research, SPEME, University of Leeds, Woodhouse Lane, Leeds LS2 9JT, U.K.

### Supporting Information

**ABSTRACT:** High-temperature superconductivity has a range of applications from sensors to energy distribution. Recent reports of this phenomenon in compounds containing electronically active BiS<sub>2</sub> layers have the potential to open a new chapter in the field of superconductivity. Here we report the identification and basic properties of two new ternary Bi–O–S compounds, Bi<sub>2</sub>OS<sub>2</sub> and Bi<sub>3</sub>O<sub>2</sub>S<sub>3</sub>. The former is non-superconducting; the latter likely explains the superconductivity at  $T_c = 4.5$  K previously reported in “Bi<sub>4</sub>O<sub>4</sub>S<sub>3</sub>”. The superconductivity of Bi<sub>3</sub>O<sub>2</sub>S<sub>3</sub> is found to be sensitive to the number of Bi<sub>2</sub>OS<sub>2</sub>-like stacking faults; fewer faults correlate with increases in the Meissner shielding fractions and  $T_c$ . Elucidation of the electronic consequences of these stacking faults may be key to the understanding of electronic conductivity and superconductivity which occurs in a nominally valence-precise compound.

Discovered in 1911, superconductivity has a wide range of applications from energy distribution to medical diagnostics, but it remains one of the most enigmatic and difficult to predict materials properties. The discovery in 2008 of a new class of high-temperature superconductors, based on two-dimensional layers of edge-sharing metal-anion tetrahedra, the “iron pnictides”,<sup>1</sup> has spurred searches for superconductivity in other layered materials.<sup>2–5</sup> Recently, there have been reports of superconductivity in Bi<sub>4</sub>O<sub>4</sub>S<sub>3</sub>,<sup>6,7</sup> LnO<sub>1–x</sub>F<sub>x</sub>BiS<sub>2</sub> (Ln = La, Ce, Pr, Nd, Yb),<sup>8–10</sup> and Sr<sub>1–x</sub>La<sub>x</sub>FBiS<sub>2</sub>,<sup>11</sup> with electronically active BiS<sub>2</sub> layers. However, the difficulty in preparing phase-pure specimens has made it challenging to unambiguously identify and study in detail the intrinsic superconducting phases.<sup>7,12</sup> Furthermore, the reported structure of Bi<sub>4</sub>O<sub>4</sub>S<sub>3</sub> is surprising on chemical grounds, containing both sulfide (S<sup>2–</sup>) and sulfate (S<sup>6+</sup>).<sup>12</sup> Herein we report the identification and structural characterization of the new compounds Bi<sub>2</sub>OS<sub>2</sub> (i.e., BiOBiS<sub>2</sub>) and Bi<sub>3</sub>O<sub>2</sub>S<sub>3</sub> [i.e., Bi<sub>6</sub>O<sub>4</sub>S<sub>4</sub>(S<sub>2</sub>)<sub>1–x</sub>S<sub>x</sub>], with the latter likely responsible for superconductivity at  $T_c = 4.5$  K.

A sample of nominal composition “Bi<sub>4</sub>O<sub>4</sub>S<sub>3</sub>” (**1**) was prepared according to literature precedent.<sup>6,7</sup> Gaseous sulfur dioxide was observed to be lost during heating, as identified by its odor and the presence of a characteristic IR absorption feature in the headspace gas of the sealed ampule at 2520 cm<sup>–1</sup>. Sample **2** was prepared similarly to **1**, but by targeting “Bi<sub>6</sub>O<sub>6</sub>S<sub>5</sub>”. A sample containing primarily Bi<sub>2</sub>OS<sub>2</sub> (**3**) was

prepared at a lower temperature by targeting “Bi<sub>12</sub>O<sub>18</sub>S<sub>11</sub>”. Low (**4**) and intermediate (**5**) stacking fault fraction specimens were prepared from **3** with additional heat treatments. Detailed synthesis procedures and crystallographic data can be found in the Supporting Information.

Initial transmission electron microscopy (TEM) investigations performed on **1** revealed the existence of at least three distinct phases: bismuth metal; a layered compound, likely of tetragonal symmetry, with lattice parameters  $a = 4.0$  Å and  $c = 20.7$  Å (primitive) or  $c = 41.4$  Å (body-centered); and a third phase that was not identified by TEM due to decomposition by the electron beam. Le Bail (unit cell only) refinements of high-resolution synchrotron X-ray diffraction (XRD) data of sample **2** (Figure 1a) are consistent with the TEM results. All sharp reflections have been indexed by a combination of Bi metal, Bi<sub>2</sub>S<sub>3</sub>, an *I*-centered tetragonal cell (hereafter “ $c = 41.4$  Å phase”), and Bi<sub>28</sub>O<sub>32</sub>(SO<sub>4</sub>)<sub>10</sub> (presumed to be the beam-sensitive phase).<sup>14</sup> However, there remain unindexed broad shoulders to several Bragg peaks. The presence of these shoulders are *hkl*-dependent and asymmetric, suggesting that the extra scattering is due not to another phase or small particle size, but rather to another kind of nanoscale structural disorder, such as stacking disorder.<sup>13</sup> Indeed, numerous stacking faults are visible in TEM images from **1** (Figure 1b). The repeat distance perpendicular to the layers averages  $d = 20$  Å for unfaulted regions, which implies that the layer stacking is along the crystallographic *c*-axis of the tetragonal cell. The faulted regions have a significantly smaller repeat distance of  $d = 13.8$  Å.

Sample **3** was prepared by heating at a lower temperature. It has a powder X-ray diffraction pattern indexable by a combination of Bi metal, Bi<sub>6</sub>O<sub>7</sub>(SO<sub>4</sub>)<sub>2</sub> [isostructural with Sb<sub>6</sub>O<sub>7</sub>(SO<sub>4</sub>)<sub>2</sub>]<sup>15</sup>, and a third phase with a primitive tetragonal unit cell of  $a = 4.0$  Å and  $c = 13.8$  Å. The *c* lattice parameter of this tetragonal cell is close to the layer spacing in faulted regions of **1**, suggesting that the faults may be small regions with the  $c = 13.8$  Å phase’s structure. This is further supported by the presence of broad features in the X-ray data of **3** in the positions expected if there were some  $c = 41.4$  Å phase stacking motifs present. The unit cell parameters of the  $c = 13.8$  Å phase are close the unit cell parameters known for CeOBiS<sub>2</sub>,<sup>16</sup> and a Rietveld refinement based on such a structural model with Bi substituted for Ce (and including the other phases present)

Received: February 1, 2013

Published: March 25, 2013

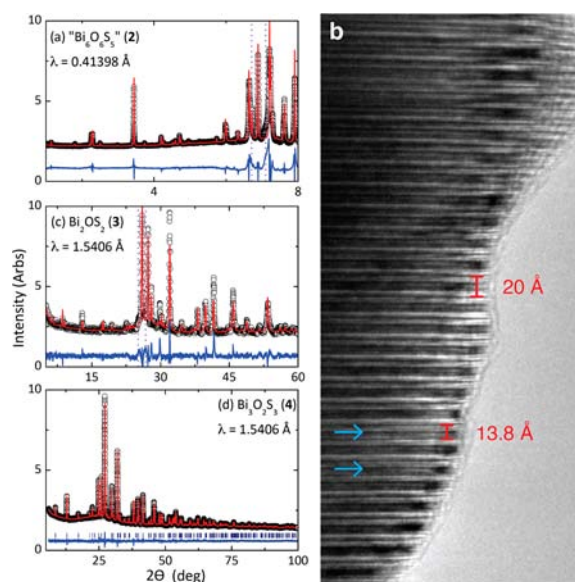


**Figure 1.** (a) Le Bail fit of synchrotron X-ray diffraction data of a sample 2. In addition to four distinct phases, including the reported “ $\text{Bi}_4\text{O}_4\text{S}_3$ ” phase, there are broad shoulders to many peaks suggestive of stacking faults or other local structure disorder.<sup>13</sup> (b) TEM micrograph of **1** showing the presence of stacking faults (indicated by arrows). (c) Rietveld refinement of **3**, predominantly the  $c = 13.8 \text{ \AA}$  stacking variant. A model derived by replacement of Ce by Bi in the known  $\text{CeOBiS}_2$  structure describes the key features of the data, although, as in (a), there are additional broad peaks. (d) Rietveld refinement of **4**, the stacking variant with  $d \approx 20 \text{ \AA}$  layer spacing.

describes the general features of the X-ray data (Figure 1c). Thus we assign the  $c = 13.8 \text{ \AA}$  phase in **3** the formula of  $\text{BiOBiS}_2$  (i.e.,  $\text{Bi}_2\text{OS}_2$ ) (Table S1), with a structure consisting of  $\text{Bi}_2\text{O}_2$  and  $(\text{BiS})_2$  layers (Figure 2a).

The structure of the  $c = 41.4 \text{ \AA}$  phase was solved in several steps. First, a sample with fewer stacking faults and containing a majority of the  $c = 41.4 \text{ \AA}$  phase, **4**, was prepared. A Rietveld refinement of the X-ray data from **4** was performed using the known structure for Bi and the reported “ $\text{Bi}_4\text{O}_4\text{S}_3$ ” structure,<sup>6</sup>

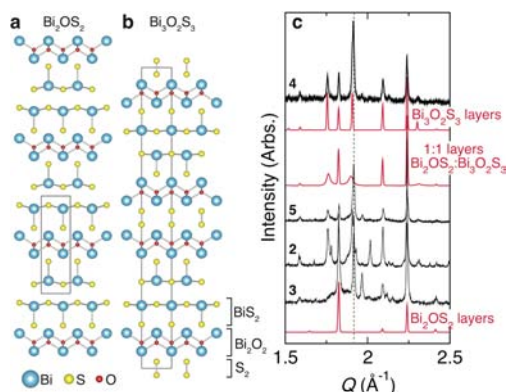


**Figure 2.** Structure representations of (a) the  $c = 13.8 \text{ \AA}$  phase,  $\text{Bi}_2\text{OS}_2$ , and (b) the  $c = 41.4 \text{ \AA}$  phase,  $\text{Bi}_3\text{O}_2\text{S}_3$ .  $\text{Bi}_2\text{OS}_2$  is built of Aurivillius-type  $\text{Bi}_2\text{O}_2$  layers alternating with  $(\text{BiS})_2$  bilayers containing two-dimensional layers of edge-sharing  $\text{BiS}_6$  octahedra. Compared to  $\text{Bi}_2\text{OS}_2$ ,  $\text{Bi}_3\text{O}_2\text{S}_3$  has every other  $(\text{BiS})_2$  bilayer replaced with  $\text{S}_2$  dimers. (c) Most samples contain mixtures of the structures in (a) and (b), giving rise to broad shoulders on some Bragg peaks. The vertical line marks the position of the strongest reflection from Bi metal.

but without the sulfate groups. The resulting Fourier difference map (Figure S5) is inconsistent with the presence of sulfates, as there is a minimum of residual electron density in the position where a maximum is expected. Further, stretching frequencies corresponding to sulfates were absent in the IR spectrum of **4** (Figure S7). Instead, the difference map suggests a mixture of  $\text{S}_2$  dimers in a  $\text{Bi}_8$  cage, and sulfide in  $\text{Bi}_4$  square planar coordination (as in  $\text{Bi}_2\text{O}_2\text{S}^{17}$ ); a mixture of these two species [i.e., any  $x$  for  $\text{Bi}_6\text{O}_4\text{S}_4(\text{S}_2)_{1-x}(\text{S})_x$ ] provides a statistically indistinguishable fit to the data. For simplicity, we assume  $\text{S}_2$  dimers in the remainder of our analysis, as they are preferred when occupancies are freely refined. The resulting fit is robust: removal of any sulfur or oxygen site from the structure, or substitution of  $\text{SO}_4$  units, results in a visibly and statistically worse fit to the data. The bond lengths and bond valence sums of this new model, containing  $\text{S}_2$  dimers and with overall formula  $\text{Bi}_3\text{O}_2\text{S}_3$  (Table S2), are physically reasonable. The structure (Figure 2b) consists of  $\text{Bi}_2\text{O}_2$  units stacked in an alternating fashion with  $(\text{BiS})_2$  and  $(\text{S}_2)$  layers. This structural variant can be derived from the structure of  $\text{Bi}_2\text{OS}_2$  by removal of  $(\text{BiS})_2$  units from between every other pair of  $\text{Bi}_2\text{O}_2$  layers. This  $\text{Bi}_3\text{O}_2\text{S}_3$  model is also consistent with TEM micrographs from the tetragonal phase in **1** (Figure S6).

We find that  $\text{Bi}_2\text{OS}_2$ -like stacking faults in  $\text{Bi}_3\text{O}_2\text{S}_3$  explain the broad extra reflections in the XRD data. Figure 2c shows simulated diffraction patterns for  $\text{Bi}_3\text{O}_2\text{S}_3$  with varying fractions of  $\text{Bi}_2\text{OS}_2$ -like regions compared to the XRD data of **2–5**. Sample **3** contains 90+% the  $\text{Bi}_2\text{OS}_2$  stacking variant. Sample **4** is predominately  $\text{Bi}_3\text{O}_2\text{S}_3$ , containing <10% of  $\text{Bi}_2\text{OS}_2$ -like stacking faults. In contrast, samples **2** and **5** contain a significant number of  $\text{Bi}_2\text{OS}_2$ -like stacking faults, approximately 40% and 20%, respectively.

Superconductivity is sensitive to the number of stacking faults. Figure 3 shows zero-field-cooled dc magnetization data

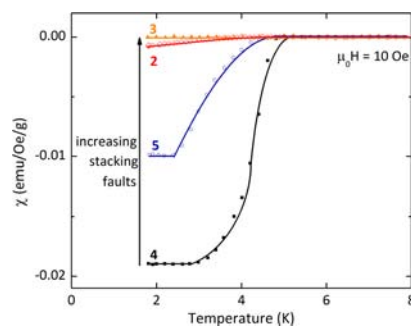


**Figure 3.** Zero-field-cooled dc magnetization data ( $\mu_0 H_{\text{appl}} = 10 \text{ Oe}$ ) of  $\text{Bi}_3\text{O}_2\text{S}_3$ - $\text{Bi}_2\text{OS}_2$  samples **4** ( $\square$ , black), **5** ( $\circ$ , blue), **2** ( $\diamond$ , red), and **3** ( $\triangle$ , orange), showing a decrease in  $T_c$  and Meissner shielding as the fraction of  $\text{Bi}_2\text{OS}_2$ -like stacking faults in  $\text{Bi}_3\text{O}_2\text{S}_3$  increases.

for **2–5**. The best superconducting signal is observed in **4**, with the magnitude sharply decreasing to **5**, **2**, and **3** as the fraction of  $\text{Bi}_2\text{OS}_2$ -like stacking faults increases and the average size and number of  $\text{Bi}_3\text{O}_2\text{S}_3$ -like regions decreases. No systematic trend with the quantity of Bi metal or other impurity phases is observed.

In conclusion, we have determined that there are at least two non-sulfate-containing phases in the Bi–O–S system,  $\text{Bi}_2\text{OS}_2$  and  $\text{Bi}_3\text{O}_2\text{S}_3$ . The former is isostructural with  $\text{CeOBiS}_2$ . The latter contains alternating layers of  $\text{Bi}_2\text{O}_2$ ,  $(\text{BiS})_2$ , and  $\text{S}_2$  dimers. The trends in physical properties imply that  $\text{Bi}_3\text{O}_2\text{S}_3$  is a superconductor with a  $T_c = 4.5 \text{ K}$ . Superconductivity

rapidly disappears as Bi<sub>2</sub>OS<sub>2</sub>-like stacking faults are introduced in Bi<sub>3</sub>O<sub>2</sub>S<sub>3</sub>. Our results bring up a number of new questions. For example: how does Bi<sub>3</sub>O<sub>2</sub>S<sub>3</sub> exhibit metallic behavior and superconductivity, which, assuming an (S<sub>2</sub>)<sup>2-</sup> electron count on the dimers, has valence-precise Bi<sup>3+</sup>? We speculate that metallicity arises either from incomplete charge transfer to S<sub>2</sub> dimers, as molecular orbital calculations, and the slightly short S–S dimer bond distance [1.8 vs the 2.0 Å expected for (S<sub>2</sub>)<sup>2-</sup>] suggest, or from partial occupancy of the cages. If true, then other factors such as the ratio of S<sub>2</sub> dimers to sulfides in the intermediary layer [i.e.,  $x$  in Bi<sub>6</sub>O<sub>4</sub>S<sub>4</sub>(S<sub>2</sub>)<sub>1-x</sub>(S)<sub>x</sub>] should also affect the structure and superconductivity.<sup>18</sup> It is now a synthetic challenge to find effective routes to prepare phase-pure specimens of compounds such as Bi<sub>3</sub>O<sub>2</sub>S<sub>3</sub>, which have multiple competing low-energy configurations, to allow us to address the fundamental structure–function relationship in this and related families of materials.

## ■ ASSOCIATED CONTENT

### 📄 Supporting Information

Complete synthetic protocols, TEM simulation, and XRD results. This material is available free of charge via the Internet at <http://pubs.acs.org>.

## ■ AUTHOR INFORMATION

### Corresponding Author

mcqueen@jhu.edu

### Notes

The authors declare no competing financial interest.

## ■ ACKNOWLEDGMENTS

This research supported by the U.S. Department of Energy (DOE), Office of Basic Energy Sciences (BES), Division of Materials Sciences and Engineering under Award DE-FG02-08ER46544. Use of the Advanced Photon Source at Argonne National Laboratory was supported by the U.S. DOE, Office of Science, BES, under Contract No. DE-AC02-06CH11357.

## ■ REFERENCES

- (1) Kamihara, Y.; Watanabe, T.; Hirano, M.; Hosono, H. *J. Am. Chem. Soc.* **2008**, *130*, 3296–3297.
- (2) Doan, P.; Gooch, M.; Tang, Z.; Lorenz, B.; Moeller, A.; Tapp, J.; Chu, P. C. W.; Guloy, A. M. *J. Am. Chem. Soc.* **2012**, *134*, 16520–16523.
- (3) Neilson, J. R.; Llobet, A.; Stier, A. V.; Wu, L.; Wen, J.; Tao, J.; Zhu, Y.; Tesanovic, Z. B.; Armitage, N. P.; McQueen, T. M. *Phys. Rev. B* **2012**, *86*, 054512.
- (4) Caron, J. M.; Neilson, J. R.; Miller, D. C.; Arpino, K.; Llobet, A.; McQueen, T. M. *Phys. Rev. B* **2012**, *85*, 180405.
- (5) Johrendt, D. *J. Mater. Chem.* **2011**, *21*, 13726.
- (6) Mizuguchi, Y.; Fujihisa, H.; Gotoh, Y.; Suzuki, K.; Usui, H.; Kuroki, K.; Demura, S.; Takano, Y.; Izawa, H.; Miura, O. *Phys. Rev. B* **2012**, *86*, 214518.
- (7) Singh, S. K.; Kumar, A.; Gahtori, B.; Shruti; Sharma, G.; Patnaik, S.; Awana, V. P. S. *J. Am. Chem. Soc.* **2012**, *134*, 16504–16507.
- (8) Mizuguchi, Y.; Demura, S.; Deguchi, K.; Takano, Y.; Fujihisa, H.; Gotoh, Y.; Izawa, H.; Miura, O. *J. Phys. Soc. Jpn.* **2012**, *81*, 114725.
- (9) Demura, S.; Mizuguchi, Y.; Deguchi, K.; Okazaki, H.; Hara, H.; Watanabe, T.; Denholme, S. J.; Fujioka, M.; Ozaki, T.; Fujihisa, H.; Gotoh, Y.; Osuke, M.; Yamaguchi, T.; Takeya, H.; Yoshihiko, T. *J. Phys. Soc. Jpn.* **2013**, *82*, 033708.
- (10) Yazici, D.; Huang, K.; White, B. D.; Chang, A. H.; Friedman, A. J.; Maple, M. B. *Philos. Mag.* **2012**, *1–8*.
- (11) Lin, X.; Ni, X.; Chen, B.; Xu, X.; Yang, X.; Dai, J.; Li, Y.; Yang, X.; Luo, Y.; Tao, Q.; Cao, G.; Xu, Z. *Phys. Rev. B* **2013**, *87*, 020504.

- (12) Kotegawa, H.; Tomita, Y.; Tou, H.; Izawa, H.; Mizuguchi, Y.; Miura, O.; Demura, S.; Deguchi, K.; Takano, Y. *J. Phys. Soc. Jpn.* **2012**, *81*, 103702.
- (13) Hendriks, S.; Teller, E. *J. Chem. Phys.* **1942**, *10*, 147–167.
- (14) Aurivillius, B. *Acta Chem. Scand. A* **1987**, *41*, 415–422.
- (15) Bovin, J.-O. *Acta Crystallogr. B* **1976**, *32*, 1771–1777.
- (16) Ceolin, R.; Rodier, N. *Acta Crystallogr. B* **1976**, *32*, 1476–1479.
- (17) Koyama, E.; Nakai, I.; Nagashima, K. *Acta Crystallogr. B* **1984**, *40*, 105–109.
- (18) Yildirim, T. *Phys. Rev. B* **2013**, *87*, 020506.